

Guanine nucleotide exchange factor RABGEF1 regulates keratinocyte-intrinsic signaling to maintain skin homeostasis

Supplemental Data

Thomas Marichal^{1,2,3,\$}, Nicolas Gaudenzio^{1,3,\$}, Sophie El Abbas^{2,†}, Riccardo Sibilano^{1,3,†}, Oliwia Zurek^{1,3,†}, Philipp Starkl^{1,3,11,†}, Laurent L. Reber^{1,3,†}, Dimitri Pirotin², Jinah Kim¹, Pierre Chambon⁴, Axel Roers⁵, Nadine Antoine⁶, Yuko Kawakami^{7,8}, Toshiaki Kawakami^{7,8}, Fabrice Bureau^{2,9}, See-Ying Tam^{1,3,*}, Mindy Tsai^{1,3,*}, & Stephen J. Galli^{1,3,10,*}

Affiliations:

¹Department of Pathology, Stanford University School of Medicine, Stanford, California 94305-5324, USA

²Laboratory of Cellular and Molecular Immunology, GIGA-Research and Faculty of Veterinary Medicine, University of Liège, 4000 Liège, Belgium.

³Sean N. Parker Center for Allergy and Asthma Research, Stanford University School of Medicine, Stanford, California 94305-5324, USA

⁴Institut de Génétique et de Biologie Moléculaire et Cellulaire (IGBMC), CNRS UMR7104/INSERM U964, Collège de France, Université de Strasbourg, 67404 Illkirch Cedex, France

⁵Institute for Immunology, Medical Faculty Carl-Gustav Carus, Technische Universität Dresden, 01307 Dresden, Germany

⁶Department of Morphology and Pathology, Laboratory of Animal Histology, Faculty of Veterinary Medicine, University of Liege, 4000 Liege, Belgium

⁷Division of Cell Biology, La Jolla Institute for Allergy and Immunology, La Jolla, California, USA

⁸Research Unit for Allergy, RIKEN Research Center for Allergy and Immunology, Yokohama, Japan

⁹WELBIO, Walloon Excellence in Life Sciences and Biotechnology, Wallonia, Belgium

¹⁰Department of Microbiology & Immunology, Stanford University School of Medicine, Stanford, California 94305-5324, USA

¹¹Present address: CeMM Research Center for Molecular Medicine of the Austrian Academy of Sciences, and Department of Medicine I, Medical University of Vienna, 1090 Vienna, Austria

Address correspondence to:

Stephen J. Galli

Department of Pathology, L-235

Stanford University School of Medicine

Center for Clinical Sciences Research

269 Campus Drive, Room 3255b

Stanford, CA 94305-5176

Tel: 650-723-7975

Fax: 650-725-6902

sgalli@stanford.edu

Mindy Tsai

Department of Pathology

Stanford University School of Medicine

Center for Clinical Sciences Research

269 Campus Drive, Room 3255a

Stanford, CA 94305-5176

Tel: (650) 736-0071

Fax: (650) 736-0073

mindyt@stanford.edu

See-Ying Tam

Department of Pathology

Stanford University School of Medicine

Center for Clinical Sciences Research

269 Campus Drive, Room 3255c

Stanford, CA 94305-5176

Tel: (650) 736-0061

Fax: (650) 736-0073

stam@stanford.edu

[§] and [†]: These authors contributed equally to this work.

^{*}: These authors are co-corresponding authors

The authors have declared that no conflicts of interest exist.

Supplemental Methods

Reagents and Antibodies

Bovine Serum Albumin (BSA), saponin, sodium citrate, tamoxifen, DMSO, DNFB, Staphylococcal enterotoxin B (SEB), dispase and corn oil were from Sigma. Mouse recombinant IL-1 β was purchased from R&D Systems. A MYD88 inhibitory peptide (i.e., a cell permeant peptide sequence that selectively blocks MYD88 homodimerization) (1) and a control peptide (i.e., an inactive and cell permeant truncated form of the MYD88 inhibitory peptide) were from Novus. *Dermatophagoides farinae* extracts (house dust mite, HDM) were purchased from Greer Laboratories. The following antibodies were obtained from Affymetrix/eBiosciences: EpCAM (CD326)-PE/Cy7 (clone G8.8), MHC-II-FITC (clone AF6-120.1), MHC-II-AlexaFluor700 (clone M5/114.15.2), CD11b-eFluor450 (clone M1/70), CD4-APC (clone GK1.5), CD3-APC (clone 17A2), c-Kit (CD117)-FITC (clone 2B8), Fc ϵ RI-PE (clone MAR-1), CD49b-APC (clone DX5), IgE-biotin (clone 23G3), Ly-6G-FITC (clone 1A8), CD45-APC-eFluor780 (clone 30-F11), F4/80-PE (clone BM8) and E-Cadherin-eFluor660 (clone DECMA-1). CD19-PE/Cy7 (clone 1D3), Streptavidin-PE/Texas Red and Annexin-V-APC were from BD Biosciences. CD11c-PE/Cy7 (clone N418) and F4/80-PE/Cy7 (clone BM8) were from Biolegend. TSLP, active caspase-3, claudin-1, Ki67, MYD88 and RABGEF1 (RABEX5) antibodies were from Abcam. K5, K6, K10, K14, loricrin and filaggrin antibodies were from Covance. Alexa594-conjugated Phalloidin, Alexa594-conjugated goat anti-rabbit, Alexa488-conjugated avidin, propidium iodide (PI) and DAPI were from Life Technologies Invitrogen. For experiments involving intracellular staining, CD4 (clone GK1.5)-FITC and Foxp3 (clone FJK-16S)-PE were from eBiosciences, and Ror γ -T (clone Q31-378)-BV786, Gata3 (clone L50-863)-BV421 and T-bet (clone O4-46)-BV650 were from BD Biosciences. For Immunoblotting, Rabex-5 (clone D21F12) rabbit mAb, phospho-IkB α (Ser32) (clone 14D4) rabbit mAb, IkB α (clone L35A5) mouse Ab, phospho-IKK α / β (clone 16A6) rabbit mAb, IKK β (clone D30C6) rabbit mAb, phospho-p44/42 MAPK (Erk1/2) (Thr202/Tyr204) rabbit Ab (#9101), p44/42 MAPK (Erk1/2) rabbit Ab (#9102), β -actin (clone 13E5) rabbit mAb and GAPDH (clone 14C10) rabbit mAb were purchased from Cell Signaling Technology.

Single-cell sorting and PCRs

Cell populations were identified as follows, after elimination of doublets and dead cells: keratinocytes (EpCAM⁺CD45⁻), skin leukocytes (EpCAM⁻CD45⁺), skin T cells (CD45⁺CD3⁺F4/80⁻), skin MCs (CD45⁺CD3⁻F4/80⁻c-Kit⁺FcεRI⁺), skin monocytes (EpCAM⁻CD45⁺F4/80⁺MHC-II⁺), blood leukocytes (CD45⁺), blood basophils (CD49b⁺IgE⁺), blood neutrophils (Gr-1⁺CD11b⁺), peritoneal B cells (CD45⁺CD19⁺), peritoneal MCs (CD45⁺c-Kit⁺FcεRI⁺). Single cells were sorted into 96-well PCR plates containing 20 µl 1x Dream Taq PCR buffer (Fermentas) and stored at -80°C. After thawing, Proteinase K (Fermentas) was added (0.25 mg/ml) and cells were incubated at 50°C for 2 h followed by inactivation of the enzyme at 95°C for 10 min. Single target PCR was performed in two rounds of amplification using nested primers in the second round. A first round of reaction contained the 3 first round primers ('F' for forward, 'M' within the loxP site, and 'R' for reverse): FP1 5'-TGTGTGCAGTGGTGGGGACTGA-3', MP1 5'-GCTCGCGAAGGCCTCTT-3' and RP1 5'-AAGGCAGCACTCCCTATGGCA-3' in a total volume of 50 µl. Then, 1 µl of the first round product was added to 2 separated second round reactions: primer FP2 5'-TATGACAGGGTTTAACCCAGGTTG C-3' combined with primer MP2 5'-AATGATCTGGGTCCTCTCCAG-3', or primer RP2 5'-TGTTGACGAGGCGTCCGAAG-3'. FP2-MP2 and FP2-RP2 detect the loxP-flanked or deleted *Rabgef1* exon 2 genomic fragments, respectively.

Skin section preparation, histology and quantification of epidermal/dermal thickness and inflammation

Mouse back skin (1 cm²) samples, ear pinnae and other organs were fixed in 10% formalin and were embedded in paraffin. 4 µm thick sections were stained with Hematoxylin & Eosin (H&E) and photographs were taken using a Nikon E1000M microscope and analyzed with Spot software 5.1 advanced. For immunostaining of mouse specimens, 4 µm thick sections were pretreated using a heat-induced epitope retrieval method (2) in 10 mM sodium citrate buffer (pH=6.0), then permeabilized for 30 min in PBS supplemented with 0.5% BSA and 0.1% saponin. Sections were 'coded' so the evaluator was not aware of their identity. For quantification of epidermal and dermal thickness, images of H&E-stained sections of back skin or ear pinnae specimens were obtained with a 10x microscope objective. For each image, eight randomly selected measurements of the distance between: i) the stratum corneum and the bottom of the basal layer, and ii) the bottom of

the basal layer and the subcutaneous adipose tissue (back skin) or the ear cartilage (ear pinnae) were recorded for quantification of: i) epidermal thickness, and ii) dermal thickness, respectively. Ear pinna cell infiltrates in the dermis between the epidermis and cartilage were counted in 3 random fixed fields per condition with a 40x microscope objective, and cell numbers were quantified per mm² of dermis.

Immunostaining and confocal microscopy

Permeabilized skin sections were incubated overnight at 4°C with primary antibodies, extensively washed, and incubated with appropriate secondary antibodies or/and Alexa488-conjugated avidin for 2 h at room temperature in the dark (see Supplemental Table 1 for the references and dilutions of antibodies used).

5 x 10⁵ shRNA-transfected keratinocytes (see below) were cultured in a sterile Nunc Lab-Tek 1.0 borosilicate cover glass system (8 chambers) in DMEM medium containing 10% FBS and Penicillin/Streptomycin (referred hereafter as complete DMEM), according to the manufacturer's protocol (CLS, Germany), at 37°C 5% CO₂. Four days later, medium was removed and cells were stained or not with PI and fixed with 4% paraformaldehyde for 20 min at room temperature. Cells were first stained for surface expression of E-cadherin or annexin-V, then permeabilized and stained for intracellular expression of polymerized actin filaments (using Phalloidin-A594) or active caspase-3 and nuclei (using DAPI).

Images were acquired using a Zeiss LSM780 Meta inverted confocal laser-scanning microscope. Images were processed using Zen software and 3-D reconstructions were performed using Imaris Bitplane software. Epidermal K6, Ki67, Claudin 1, Filaggrin, RABGEF1 and MYD88 mean fluorescence intensities were analyzed using the "measurement function" of ImageJ software on randomly chosen epidermal areas of identical size (i.e., same total number of pixels).

Bacterial CFU counts

Blood (100 µl) was collected, and liver, kidneys, spleen and a back skin specimen (1 cm²) were excised and homogenized in 1 ml PBS. Samples were serially diluted in PBS and plated in duplicate on Tryptic Soy Agar (Oxoid LTD). Plates were incubated overnight at 37°C to enumerate colony forming units (CFUs) the next day. Data show total CFUs per organ.

***In vitro* keratinocyte culture and shRNA-mediated RABGEF1 knock down**

PDV mouse keratinocytes (3) were cultured in complete DMEM according to the manufacturer's protocol (CLS). *E. coli*-amplified Suresilencing shRNA plasmids from Qiagen were used. PDV keratinocytes were stably transfected using Attractene reagent (Qiagen) with 1.2 µg DNA of *Rabgef1* Suresilencing shRNA plasmids or negative control shRNA plasmids (i.e., a scrambled artificial sequence which does not match any mouse gene) (Qiagen, Cat# KR52575P) containing a puromycin resistance gene in 6-well plates, for 48 h in complete DMEM. Transfected cells were then transferred into complete DMEM containing 4µg/ml puromycin and selected for puromycin resistance for 6 weeks. Suppression of the protein produced by the targeted gene was verified by Western blot. When the cells reached 80% confluence, control shRNA- and *Rabgef1* shRNA-transfected keratinocytes were collected for Western blot studies, and cell culture supernatants were assayed for IL-1β levels by ELISA (R&D Systems). Alternatively, cells were stimulated with recombinant mouse IL-1β (50 ng/ml for 5, 15, 30 or 60 minutes) for Western blot studies.

RNA isolation and mRNA expression analyses

Back skin samples (1 cm²) were collected from the same anatomical location in 7 week-old female *Rabgef1*^{K-KO} and control mice (at the center of the back, behind the shoulders). Tissue RNA was isolated using Trizol (Life Technologies) and transcribed into cDNA using the High Capacity cDNA Reverse Transcription Kit (Applied Biosystems).

Gene expression analysis was performed using microarrays (Affymetrix Mouse Genome 430 2.0 array), with two replicates per genotype. Microarray data were analysed using Bioconductor for R (4). Briefly, raw data were background-corrected and quantile-normalized using the Robust Multichip Average (RMA) algorithm of package 'oligo' in Bioconductor. Probes were annotated by using the annotation package "mouse4302.db". Differential expression analysis was performed using Linear Models for Microarray Data (Limma) package in Bioconductor. A list of 760 differentially expressed genes between *Rabgef1*^{K-KO} and control skin was obtained using thresholds as following: Benjamini Hochberg adjusted *P* value (adj *P* value) < 0.01 AND Fold Change (FC) > 2 or < 0.5, and after having filtered out non-annotated probes. A volcano plot was obtained by plotting log₂ (FC) on the x axis and -log₁₀ (adj *P* value) on the y axis for all probes present in the Affymetrix Mouse Genome 430 2.0 array, including non-annotated ones. Points beyond thresholds for differential expression were highlighted in red (adj *P* value < 0.01 AND FC

> 2) or blue (adj *P* value < 0.01 AND FC < 0.5). A heatmap of the 760 annotated differentially expressed probes was obtained by using *heatmap.2* function of package ‘gplots’ in R. *Rowv* and *Colv* arguments were set to ‘TRUE’ in order to allow dendrogram constructions for both samples and genes. Microarray data have been deposited in Array Express public database, accession number E-MTAB-5000 (<http://www.ebi.ac.uk/arrayexpress/experiments/E-MTAB-5000>).

For real time PCRs, target gene Ct levels (primer sequences available in Supplemental Table 2) were normalized to the housekeeping gene *Eef1b2* in the same sample. Relative gene expression compared to healthy controls was calculated using the $2^{-\Delta\text{Ct}}$ algorithm.

Gene Set Enrichment Analysis (GSEA)

GSEA between Rabgef1^{K-KO} skin and MsigDB hallmark gene sets

In order to identify biological signatures enriched in *Rabgef1^{K-KO}* skin compared to control skin, and vice-versa, we employed the non-parametric, rank-based tool, Gene Set Enrichment Analysis (GSEA version 2.2.2) (5). Normalized microarray data from *Rabgef1^{K-KO}* and control skin samples were used by GSEA as dataset to rank genes between the two phenotypes. Since: (i) each class (*Rabgef1^{K-KO}* and control samples) contains 2 samples, and (ii) RMA normalized data are in log scale, « Diff_of_Classes » method was chosen to rank genes in the dataset. Enrichment analysis was then performed using hallmark gene sets of MsigDB database.

Similarity analysis of Rabgef1^{K-KO} and HDM/SEB models (GSE53132)

We used GSEA to search for gene expression similarity between our *Rabgef1^{K-KO}* model and a mouse model of AD in which repeated epicutaneous applications of HDM and SEB induced eczematous skin lesions (GSE53132)(6). Microarray expression data were first obtained from Gene Expression Omnibus (GEO) repository by using the *getGEO* function of package ‘GEOquery’ in Bioconductor. Data from healthy and AD-induced C57BL/6 mice were then used in GSEA to rank genes using « Diff_of_Classes » method, and enrichment analysis was performed using two gene sets: (i) upregulated genes in *Rabgef1^{K-KO}* compared to Controls (adj *P* value < 0.01 AND fold change [FC] > 2), and (ii) upregulated genes in controls compared to *Rabgef1^{K-KO}* (adj *P* value < 0.01 AND FC > 2).

Similarity analysis of Rabgef1^{K-KO} and human AD skin samples

We used GSEA to test for an enrichment of our *Rabgef1^{K-KO}* differentially expressed genes in four AD human transcriptomic datasets (GSE5667, GSE36842, GSE6012 and GSE65832). The

approach was the same for GSE5667, GSE36842 and GSE6012: (i) expression datasets were first ranked between 2 phenotypes (lesional AD vs normal skin for GSE5667, acute AD vs chronic AD for GSE36842 and active AD vs normal skin for GSE6012) using the « Signal2Noise » method, and (ii) enrichment analysis was performed using the two *Rabgef1^{K-KO}* gene sets described in the section above: "*Similarity analysis of Rabgef1^{K-KO} and HDM/SEB models (GSE53132)*".

RNA-Seq data from GSE65832 were treated differently, following recommendations of GSEA tutorial for RNA-Seq data: (i) processed data were directly uploaded from GEO as a text file containing FC and adj *P* values, (ii) the list of genes was preranked using log₂FC values between lesional and non lesional AD, and (iii) enrichment analysis was performed using GSEA Preranked mode.

The characteristics of AD patients and healthy controls whose skin gene expression profiles were analyzed and compared to those of *Rabgef1^{K-KO}* and control mice are presented in Supplemental Table 3.

Immunoblotting

Cells were lysed in Pierce IP Lysis Buffer (Pierce) supplemented with Halt Protease Inhibitor Cocktail (Thermo Scientific) and Halt Phosphatase Inhibitor Cocktail (Thermo Scientific) and the resulting lysates were separated by 10% SDS-PAGE and then electroblotted onto Invitrolon PVDF membranes (Novex, Life Technologies). Membranes were blocked in 5% nonfat dry milk in Tris-buffered saline-Tween 20 (0.1%) buffer and then probed with primary antibody in 5% BSA-Tris-buffered saline-Tween 20 (0.1%) buffer. The antigen-antibody complexes were visualized using horseradish peroxidase-conjugated secondary antibody to rabbit or mouse IgG (Cell Signaling Technology) with SuperSignal West Pico Chemiluminescent Substrate Kit (Thermo Scientific) and the images were detected by exposing membranes to autoradiography films (GeneMate). The exposed films were scanned and specific signals were quantified by UN-SCAN-IT gel Version 5.3 (Silk Scientific).

Transmission Electron Microscopy

For ultrastructural analysis, adherent keratinocytes that reached 80% confluence were pre-fixed in the culture plate for 2 min in a 2.5% (w/v) glutaraldehyde solution in 0.1 M cacodylate buffer (pH 7.4). Cells were rinsed with the same buffer, scraped from the plate and centrifuged. The pellet was

post-fixed for 30 min in a 2/3 w/w mix of OsO₄ and K₄Fe(CN)₆ in a 0.1 M cacodylate buffer (pH 7.4), dehydrated in a graded series of ethanol baths and embedded in EPON 812 (Fluka), according to standard procedures. The resin specimen blocks were trimmed and ultrathin-sections of 70-90 nm of selected areas were cut, collected on copper grids and contrasted with 1% (w/v) uranyl acetate before examination with a Zeiss EM910 transmission electron microscope (Zeiss). The numbers of dense TJs were determined blindly by a trained histologist, and the areas of intercellular spaces were quantified blindly using ImageJ software and were normalized against the length of surface contact between adjacent cells.

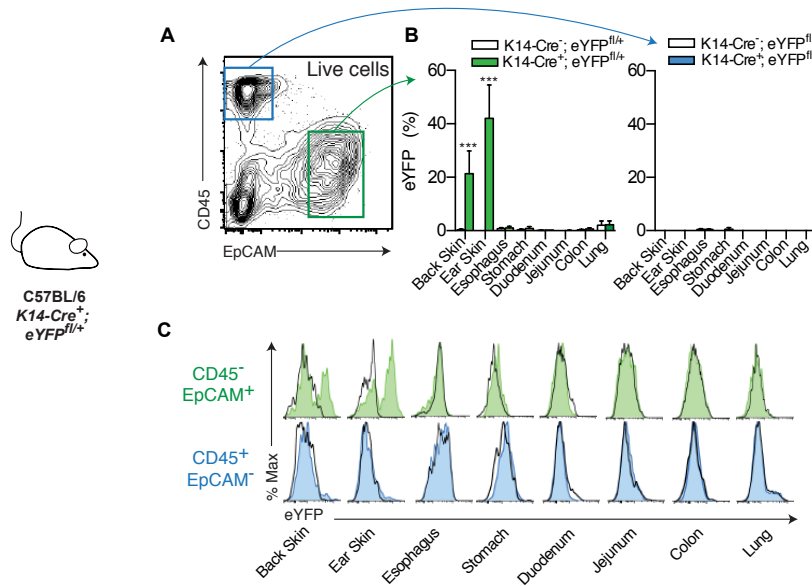
Mouse model of HDM/SEB-induced AD

Dermatitis was induced in C57BL/6 mice as previously described (6, 7) (Fig. 8A). Briefly, back skin was shaved and a solution of 500 ng of Staphylococcal enterotoxin B (SEB, Sigma-Aldrich) and of 10 µg of *Dermatophagoides farina* extract (HDM, Greer Laboratories) in PBS was applied on a gauze pad placed on the shaved back and occluded with a Tegaderm™ Transparent Dressing (3M HealthCare). Three days later, the gauze pads were replaced. Four days later, dressings were removed and mice were kept without treatment for the next week. This "3 + 4" days pattern of treatment was repeated two more times, so that the mice were subjected to three cycles of such treatment. Two days after the last cycle of treatment, the mice were euthanized and back skin specimens were obtained for immunohistological analyses.

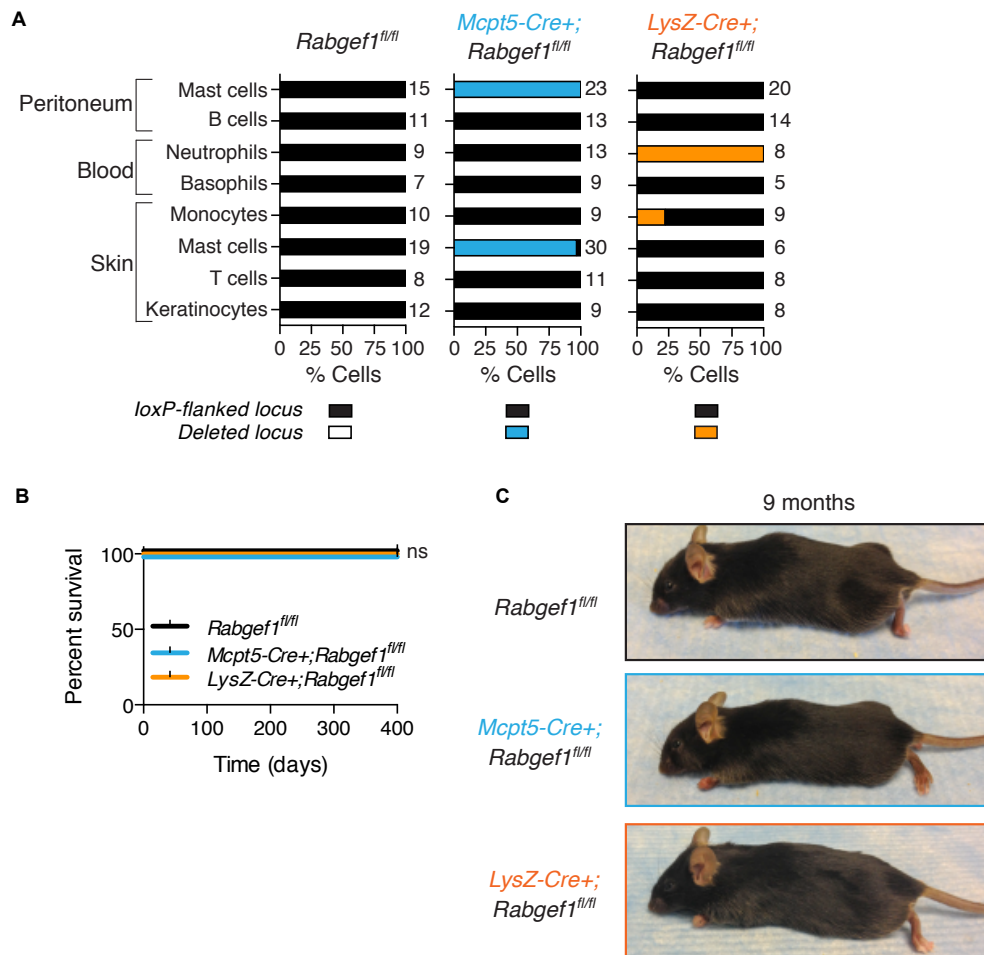
Supplemental References

1. Benedetti F, Davinelli S, Krishnan S, Gallo RC, Scapagnini G, Zella D, and Curreli S. Sulfur compounds block MCP-1 production by Mycoplasma fermentans-infected macrophages through NF-kappaB inhibition. *J Transl Med.* 2014;12(145).
2. Gaudenzio N, Laurent C, Valitutti S, and Espinosa E. Human mast cells drive memory CD4+ T cells toward an inflammatory IL-22+ phenotype. *J Allergy Clin Immunol.* 2013;131(5):1400-7 e11.
3. Caulin C, Scholl FG, Frontelo P, Gamallo C, and Quintanilla M. Chronic exposure of cultured transformed mouse epidermal cells to transforming growth factor-beta 1 induces an epithelial-mesenchymal transdifferentiation and a spindle tumoral phenotype. *Cell Growth Differ.* 1995;6(8):1027-35.
4. Gentleman RC, Carey VJ, Bates DM, Bolstad B, Dettling M, Dudoit S, Ellis B, Gautier L, Ge Y, Gentry J, et al. Bioconductor: open software development for computational biology and bioinformatics. *Genome Biol.* 2004;5(10):R80.
5. Subramanian A, Tamayo P, Mootha VK, Mukherjee S, Ebert BL, Gillette MA, Paulovich A, Pomeroy SL, Golub TR, Lander ES, et al. Gene set enrichment analysis: a knowledge-based approach for interpreting genome-wide expression profiles. *Proc Natl Acad Sci U S A.* 2005;102(43):15545-50.
6. Kawakami Y, Yumoto K, and Kawakami T. An improved mouse model of atopic dermatitis and suppression of skin lesions by an inhibitor of Tec family kinases. *Allergol Int.* 2007;56(4):403-9.
7. Ando T, Matsumoto K, Namiranian S, Yamashita H, Glatthorn H, Kimura M, Dolan BR, Lee JJ, Galli SJ, Kawakami Y, et al. Mast cells are required for full expression of allergen/SEB-induced skin inflammation. *J Invest Dermatol.* 2013;133(12):2695-705.

Supplemental Figures



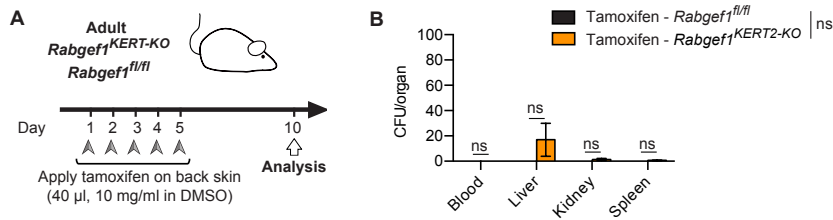
Supplemental Figure 1. Efficiency and specificity of K14-Cre activity using *K14-Cre*⁺; *eYFP*^{fl/+} reporter mice. *K14-Cre*⁺ mice were crossed to the Cre excision reporter mice R26R-eYFP, and eYFP expression was assessed by flow cytometry in CD45⁻EpCAM⁺ epithelial cells and CD45⁺EpCAM⁻ leukocytes isolated from the indicated organs. (A) Representative dot plot of singlet living cells according to CD45 and EpCAM expression after tissue enzymatic digestion. (B) Bar graphs showing % of eYFP⁺ CD45⁻EpCAM⁺ cells (green, left panel) and CD45⁺EpCAM⁻ cells (blue, right panel) in the indicated organs. Results are shown as mean+SD and are pooled from 3 independent experiments (n=6-8 mice/group). *P* values were calculated by two-tailed unpaired Student's *t* test. ***, *P*<0.001. (C) Representative histograms of eYFP expression in CD45⁻EpCAM⁺ cells (green, top panels) and CD45⁺EpCAM⁻ cells (blue, bottom panels) isolated from the indicated organs.



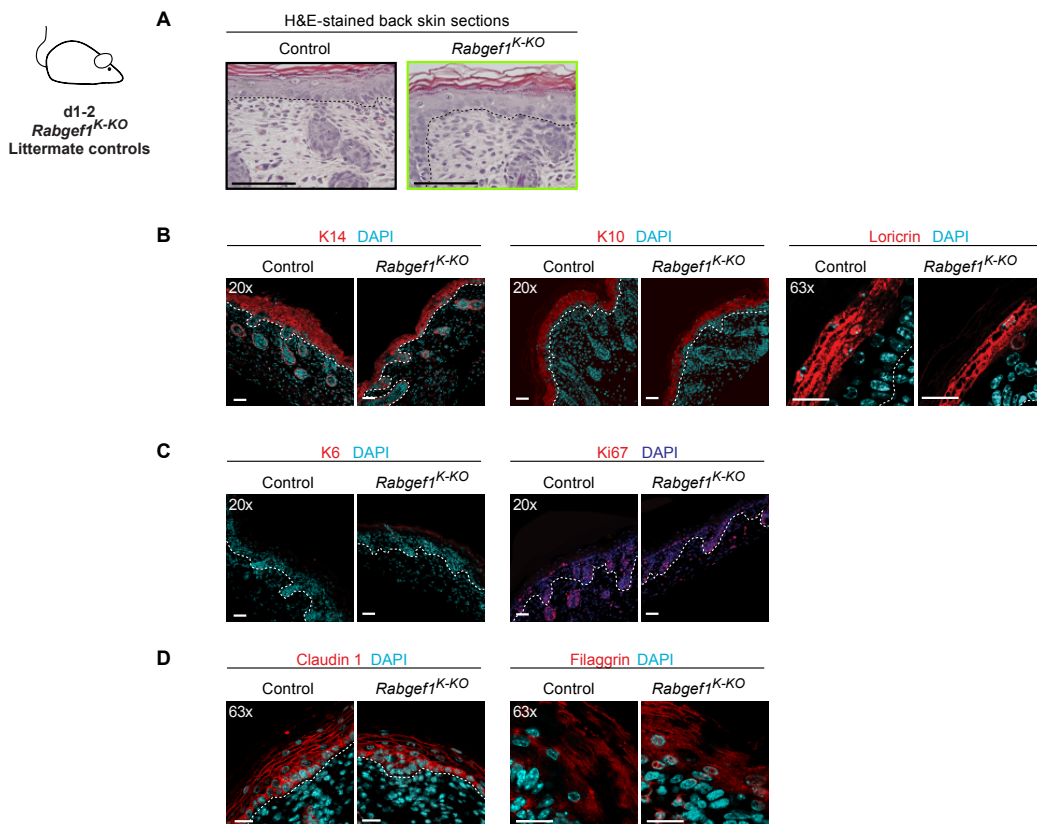
Supplemental Figure 2. Phenotype of mice with mast cell- or 'myeloid'-restricted *Rabgef1* deletion. (A) Specificity and efficiency of *Rabgef1* gene deletion assessed by single cell PCR detection of loxP-flanked or deleted *Rabgef1* exon 2 genomic fragments; inserts indicate the number of products analyzed/cell type; results are pooled from 2 sorting experiments. (B) Survival of *Mcpt5-Cre+; Rabgef1^{fl/fl}*, *LysZ-Cre+; Rabgef1^{fl/fl}*, and *Cre-; Rabgef1^{fl/fl}* mice over time (n=10 mice/group). *P* values are versus littermate controls and were calculated by Mantel-Cox test. (C) Representative photographs of mice from the indicated genotype at the age of 9 months. ns, not significant.



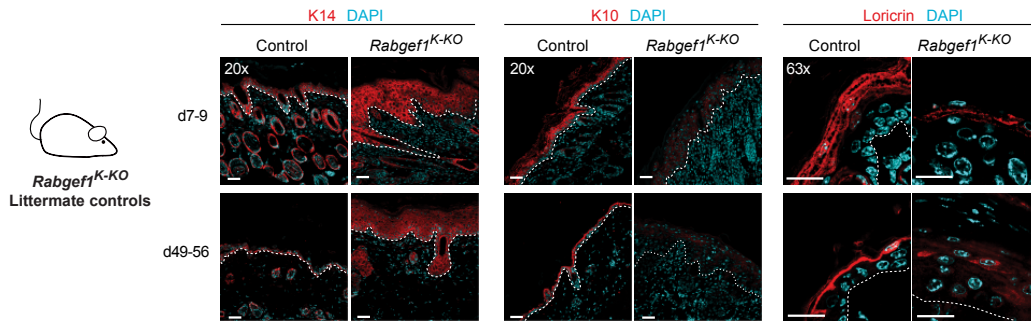
Supplemental Figure 3. Absence of histological abnormalities in several organs from adult *Rabgef1^{K-KO}* mice. (A-K) Histological pictures of the indicated organs at d49-56, at a time when the surviving *Rabgef1^{K-KO}* mice have an appearance similar to that shown in Figure 1E and are close to death. Pictures are representative of 4 analyzed samples (from 4 different mice)/group. Original magnification is shown in the upper right corner. Scale bars: 100 or 500 μm , as indicated in the photos.



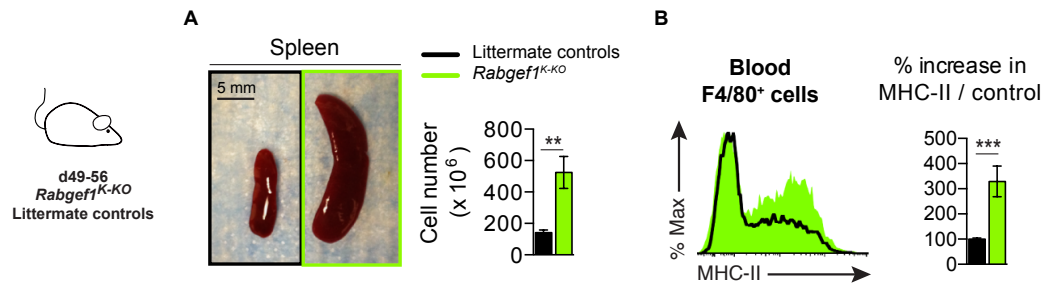
Supplemental Figure 4. Bacterial counts in the blood, liver, kidney and spleen of tamoxifen-treated *Rabgef1*^{KERT-KO} and control mice. (A) Experimental outline. By day 10 of the protocol, the tamoxifen-treated *Rabgef1*^{KERT-KO} mice exhibited extensive skin pathology whereas the identically-treated *Rabgef1*^{fl/fl} mice appeared to be normal. (B) Bar graph shows the numbers of bacterial Colony Forming Units (CFU) per ml of blood or per organ. Results are shown as mean \pm SEM and are pooled from 2 independent experiments (n=3-5 mice/group). *P* values were calculated using a two-way ANOVA followed by Tukey's test for multiple comparisons. ns, not significant.



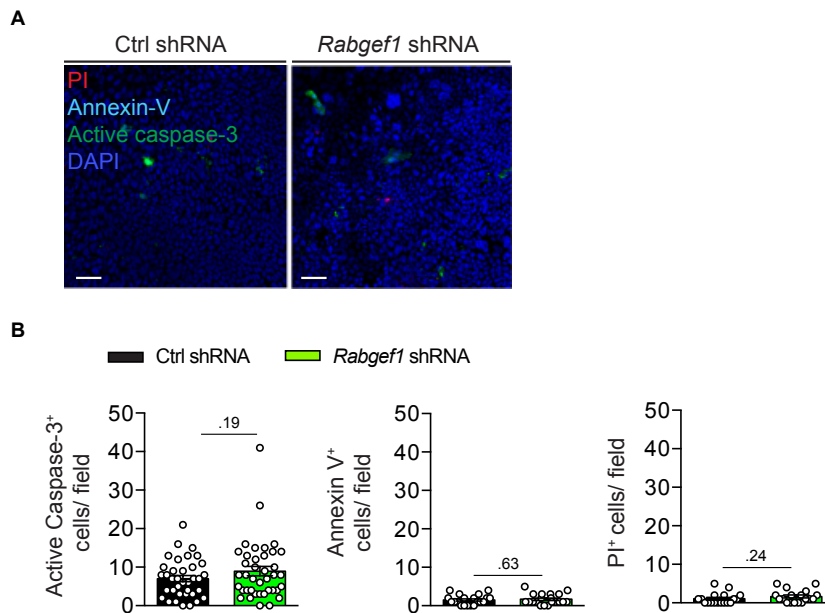
Supplemental Figure 5. Skin histology and confocal microscopy analysis of keratinocyte-associated proteins in newborn (d1-2) *Rabgef1^{K-KO}* mice. Comparison between d1-2 *Rabgef1^{K-KO}* and control mice. **(A)** Representative H&E staining of back skin sections. **(B-D)** Representative confocal microscopy pictures of back skin sections with the indicated staining. Pictures are representative of 4 or 5 samples (from 4-5 different mice)/group, each giving similar results. Dashed lines identify the dermal-epidermal junction. Scale bars: 50 μm ; original magnification: 20x or 63x, as indicated.



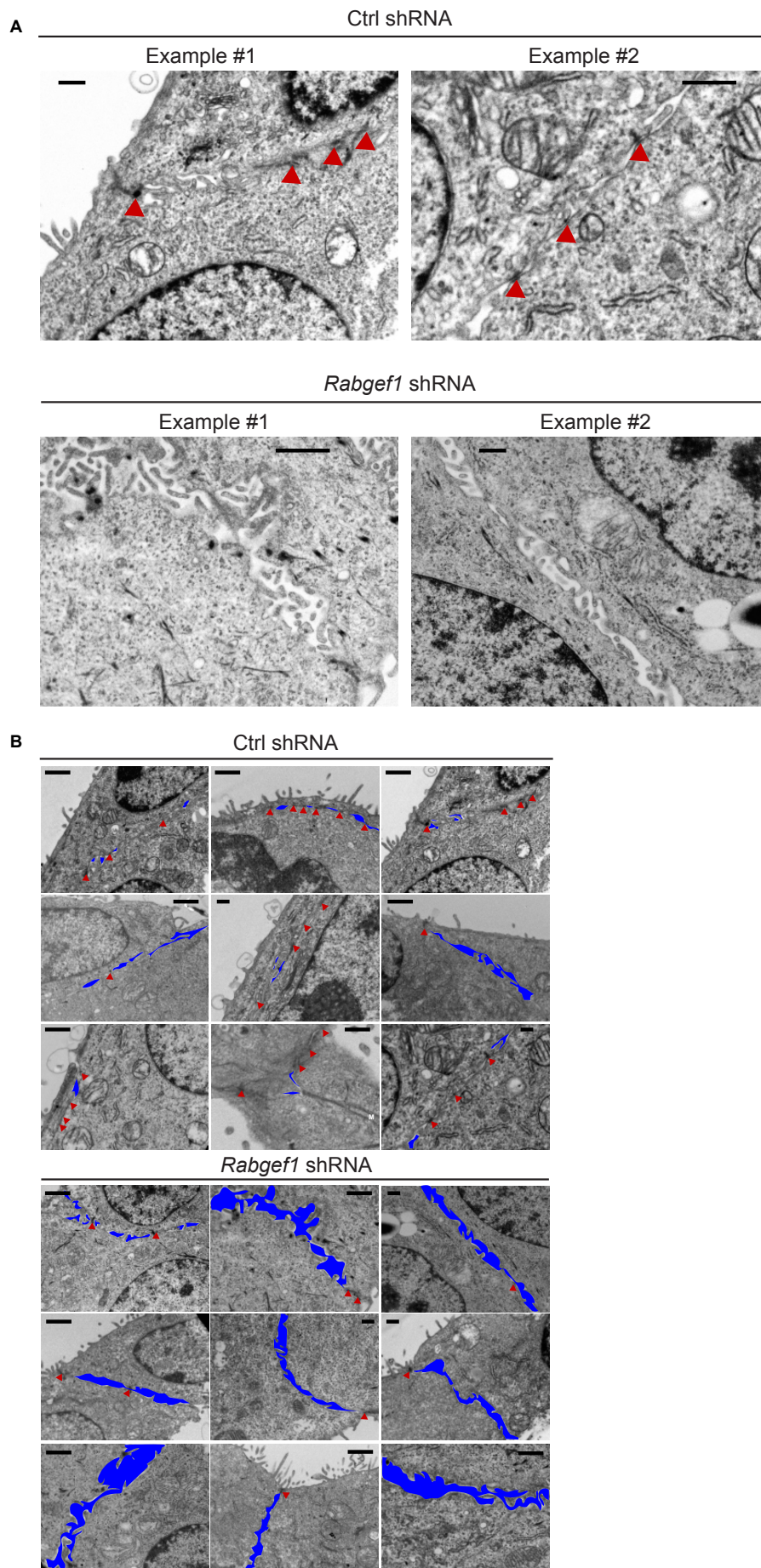
Supplemental Figure 6. Keratinocyte-associated proteins in the skin of *Rabgef1^{K-KO}* mice. Representative confocal microscopy pictures of back skin sections from d7-9 (upper panel) or adult (lower panel) *Rabgef1^{K-KO}* and control mice with the indicated staining (red) merged with DAPI (blue). Pictures are representative of 4 or 5 analyzed skin samples (from 4-5 different mice)/group. Dashed lines identify the dermal-epidermal junction. Scale bar: 50 μm ; original magnification: 20x or 63x, as indicated.



Supplemental Figure 7. Splenomegaly and increased MHC-II expression in blood monocytes of adult *Rabgef1^{K-KO}* mice. (A) Representative pictures of spleens from adult *Rabgef1^{K-KO}* and control mice; bar graph shows quantification of spleen cell numbers (n=2-5 mice/group). (B) Flow cytometry analysis of blood monocytes from adult *Rabgef1^{K-KO}* and control mice for MHC-II expression; bar graph shows the quantification of the % increase in MFI in *Rabgef1^{K-KO}* vs. control mice (n=3-6 mice/group). Results are shown as mean \pm SEM. *P* values were calculated by two-tailed unpaired Student's *t* test. **, *P*<0.01, ***, *P*<0.001. MFI, Mean Fluorescence Intensity.

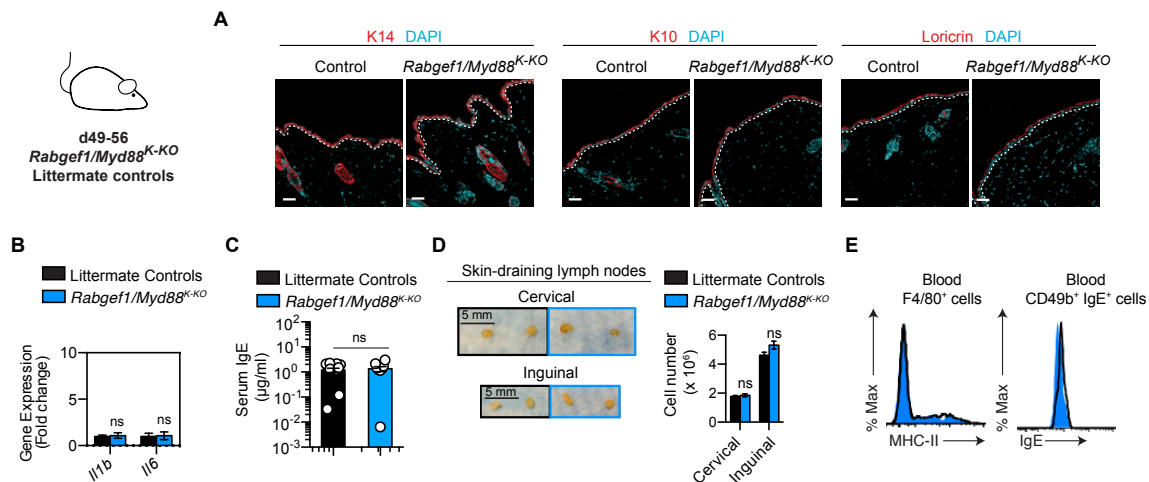


Supplemental Figure 8. Assessment of apoptosis and necrosis in RABGEF1-deficient keratinocytes. (A) Representative confocal microscopy pictures of propidium iodide (PI, red), annexin-V (cyan), active caspase-3 (green) staining merged with DAPI (blue) in control (Ctrl) shRNA-transfected or *Rabgef1* shRNA-transfected mouse keratinocytes. (B) Bar graphs show quantification of active caspase-3, annexin-V and PI positive cells. Results are shown as mean±SEM and are pooled from 2 independent experiments generated with 2 different batches of cells. *P* values were calculated by two-tailed unpaired Student's *t* test. Scale bars: 50 μ m.

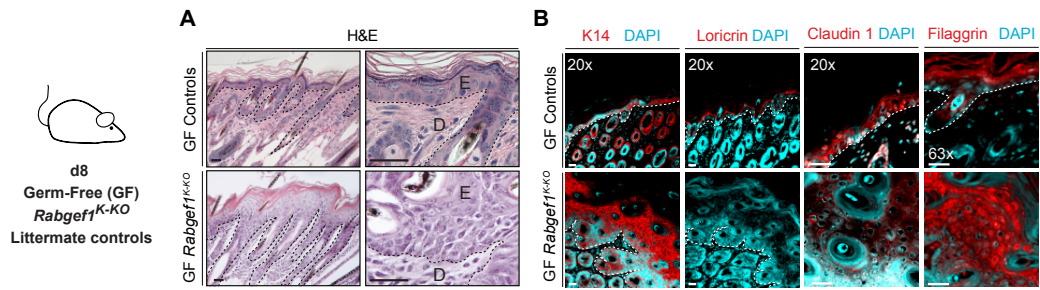


Supplemental Figure 9. Ultrastructural abnormalities of RABGEF1-deficient keratinocytes.

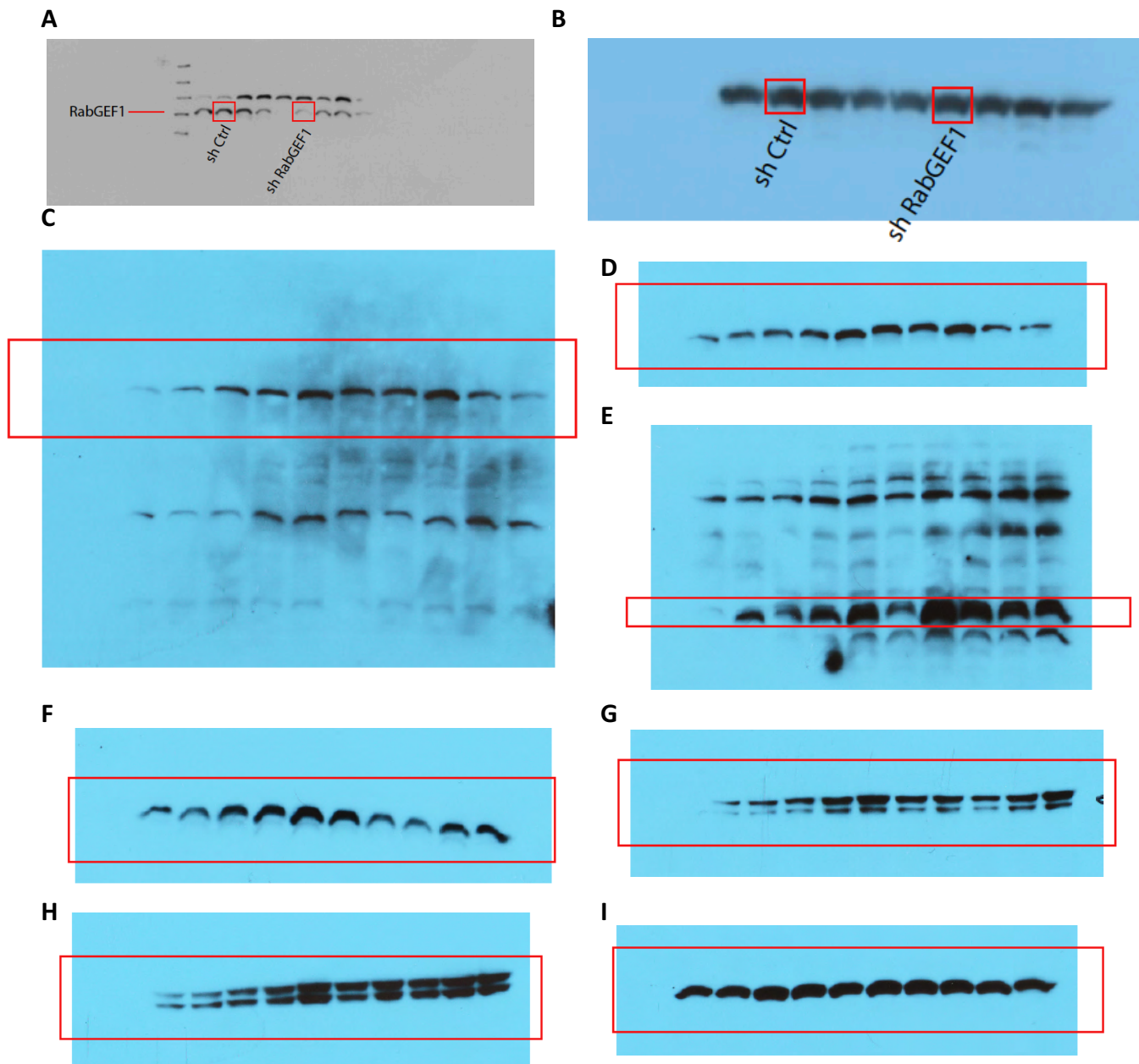
Original transmission electron microscopy pictures of control (Ctrl) shRNA-transfected or *Rabgef1* shRNA-transfected mouse keratinocytes *in vitro* (**A**) that are also shown with colored labeling in Figure 5E and (**B**) that have been used for the quantification of TJ numbers and intercellular spaces shown in Figure 5, F and G. Red arrows indicate TJs (identified as dense sites with a close apposition between adjacent membranes) and blue areas are intercellular spaces. Scale bars: 250 nm; original magnification: 6300x.



Supplemental Figure 10. Phenotype of *Rabgef1/Myd88^{K-KO}* mice. *Rabgef1/Myd88^{K-KO}* and control mice are compared. (A) Representative confocal microscopy pictures of back skin sections with the indicated staining. (B) RT-qPCR mRNA expression analysis of *Il1b* and *Il6* in back skin specimens (n=5 mice/group). (C) Serum IgE concentrations (n=9-14 mice/group). (D) Representative pictures of skin draining lymph nodes; bar graph shows numbers of lymph node cells (n=8 mice/group). Results are shown as mean±SEM. (E) Flow cytometry analysis of MHC-II and IgE expression of blood monocytes and basophils respectively, from adult *Rabgef1/Myd88^{K-KO}* and control mice. Results are representative of 4 analyzed mice/group. *P* values are versus controls and were calculated by two-tailed unpaired Student's *t* test. Dashed lines identify the dermal-epidermal junction. Scale bars: 50 µm; ns, not significant.



Supplemental Figure 11. Skin histology and confocal microscopy analysis of keratinocyte-associated proteins in d8 Germ-Free (GF) *Rabgef1*^{K-KO} mice. Comparison between d8 GF *Rabgef1*^{K-KO} and GF control mice. **(A)** Representative H&E staining of back skin sections. **(B)** Confocal microscopy pictures of back skin sections with the indicated staining. Dashed lines identify the dermal-epidermal junction. Scale bar: 50 μ m; original magnification: 20x, except for Filaggrin: 63x. D, dermis; d, day; E, epidermis.



Supplemental Figure 12. Full unedited gels of blots shown in Figure 4F and 4G. (A) RABGEF1 protein shown in Figure 4F. **(B)** GAPDH protein shown in Figure 4F. **(C)** p-IKK α/β shown in Figure 4G. **(D)** Total IKK β shown in Figure 4G. **(E)** p-I κ B α shown in Figure 4G. **(F)** Total I κ B α shown in Figure 4G. **(G)** p-ERK shown in Figure 4G. **(H)** Total ERK shown in Figure 4G. **(I)** β -actin shown in Figure 4G.

Supplemental Tables

Antibody	Company	Cat#	Dilution
Primary antibodies			
Anti-TSLP	Abcam	ab47943	1:50
Anti-active caspase-3	Abcam	ab13847	1:50
Anti-claudin-1	Abcam	ab15098	1:50
Anti-MYD88	Abcam	ab2064	1:50
Anti-RABEX-5 (RABGEF1)	Abcam	ab113480	1:50
Anti-Ki67	eBioscience	14-5698-80	1:50
Anti-K6	Covance	PRB-169P	1:50
Anti-K10	Covance	PRB-155P	1:50
Anti-K14	Covance	PRB-159P	1:50
Anti-Filaggrin	Covance	PRB-417P	1:50
Anti-Loricrin	Covance	PRB-145P	1:50
Secondary antibodies			
Goat anti-Rabbit Alexa456	Life technologies	A11035	1:200
Goat anti-Rat Alexa647	Life technologies	A21247	1:200

Supplemental Table 1. List of antibodies used for immunofluorescence studies of mouse and human skin specimens.

Target	Forward Primer (5' → 3')	Reverse Primer (3' → 5')
<i>Cldn1</i>	TCGACTCCTTGCTGAATCTGA	TCATCTTCCAGGCACCTCAT
<i>Ifng</i>	TGAGGTCAACAACCCACAGG	TTCCGCTTCCTGAGGCTGGA
<i>Il1b</i>	GCTTCCTTGTGCAAGTGTCTGAA	GAACAGGTCATTCTCATCACTGTCA
<i>Il1r1</i>	GCACGCCCAGGAGAATATGA	AGAGGACACTTGCGAATATCAA
<i>Il13</i>	TATTGAGGAGCTGAGCAACATCAC	TCTGGGTCTGTAGATGGCA
<i>Il17a</i>	GAGAGCTTCATCTGTGTCTCTGAT	TCAGTGTTTGGACACGCTGAGCT
<i>Il22</i>	CGATCTCTGATGGCTGTCCT	ACGCAAGCATTCTCAGAGA
<i>Il4</i>	GTCCTCACAGCAACGAAGAACACCA	CTCATTCATGGTGCAGCTTATCGA
<i>Il5</i>	TCACCGAGCTCTGTTGACAA	CCACACTTCTTTTTTGGCG
<i>Ccl3</i>	CTCTGTACCATGACACTCTGCA	CTCTTAGTCAGGAAAATGACACCTG
<i>Cxcl2</i>	CGCTGTCAATGCCTGAAGAC	AACTCAAGCTCTGGATGTTCTTG
<i>Cxcl3</i>	AATGAGCTGCGCTGTCAGTGCCTG	ACCATTCTTGAGTGTGGCTATGACT
<i>Eef1b2</i>	AGAGCTACATTGAGGGGTACGT	GACTTGATGTGATTATACCAACGTAG
<i>Flg</i>	TGGAAGGACAACACTACAGGCA	TGGAAGGACAACACTACAGGCA
<i>Krt6b</i>	AGCTACTCCTATGGCAGCAG	TGATGGTGGGAAGAGCTGAGG
<i>Mki67</i>	GGGTTTCCTTCAGCAAGCCT	GGCATTCCCTCACTCTTGTT

Supplemental Table 2. Sequences of primers used for quantitative RT-PCR expression analyses.

	Specimens	n	Patient characteristics	Clinical diagnosis AD (criteria employed)		Medications	Biopsy
GSE5667	Lesional AD	6	<i>Not available</i>	YES	>= 4 criteria among: associated pruritus, typical morphology and distribution, chronic or chronically relapsing course, early onset (<5 years of age), personal or family history of atopic (i.e. elevated allergen-specific IgE or history of asthma, allergic rhinitis, or AD), generally dry skin.	No non-prescribed medications (e.g. aspirin), no other systemic treatments (e.g. antihistamines), no alcoholic beverages the week before biopsy, no topical medications on biopsy site for >7 days, no skin infection, no oral corticosteroids.	No scratching, no UV light the week before biopsy; 6-mm diameter punch biopsy: no pronounced lichenification.
	Normal Skin	5	<i>Not available</i>	Non-atopic subjects.		<i>Info not available</i>	6-mm diameter punch biopsy.
GSE6012	Active AD	10	Caucasian origin; 2 males and 8 females; Age: median 40.3 years, range 21-50.	YES: moderate-to-severe AD.	Severity Scoring of Atopic Dermatitis (SCORAD) index (0-103): median 42.6, range 20.6-60. IgE levels: median 1400 kU/l, range 150-14400 kU/l.	No local or systemic treatment with glucocorticoids or tacrolimus within 2 weeks.	4-mm diameter punch biopsy.
	Normal Skin	10	Caucasian origin; 2 males and 8 females; Age: median 43 years, range 25-50.	Non-AD non-allergic subjects.	Symptom-free, no history of AD or any other atopic or chronic disease; IgE levels: median 24.5 kU/l, range 8-65 kU/l.	<i>Not available</i>	4-mm diameter punch biopsy.
GSE36842	Acute AD	8 ^s	Family history of atopy in 2/8 patients; 4 males and 6 females; Age: median 44 years, range 20-67 years; no <i>FILAGGRIN</i> gene mutations found.	YES: moderate-to-severe AD.	SCORAD index: mean 50, range 40-63. IgE levels: mean 1032 kU/l, range 27.9-3652 kU/l (reference range 0-160 kU/l).	<i>Not available</i>	4-6 mm diameter punch biopsy; new lesions of less than 72 hours duration; lack of skin lichenification; lack of regenerative hyperplasia (<150 µm epidermal thickness on H&E-stained sections).
	Chronic AD						4-6 mm diameter punch biopsy; lesions of >72 hours duration.
GSE65832	Lesional AD	20	12 males and 8 females; Age: median 46, range 18-69.	YES: moderate-to-severe AD.	At least 10% body surface area involvement; SCORAD index: median 58.5, range 44-97; Serum IgE levels: median 745 kU/l, range 3.6-70530.	Off of all treatment for at least 4 weeks.	6-mm diameter punch biopsy.
	Non lesional AD						6-mm diameter punch biopsy.

Supplemental Table 3. Characteristics of AD patients whose skin gene expression profiles were analyzed and compared to those of *Rabgef1*^{KO} and control mice in Table 3. ^s: For each of the 8 patients, the analysis included data from biopsies of both acute and chronic lesions.

PATIENT	Age	Gender	Location	CLINICAL FEATURES	HISTOLOGICAL DIAGNOSIS	CLINICAL DIAGNOSIS
1	63	M	ELBOW	Rash, bilateral dorsal hands and elbows	SPONGIOTIC DERMATITIS	Atopic dermatitis
2	53	F	LEFT ARM	History of eczema with itchy rash on arms and legs	SPONGIOTIC DERMATITIS WITH EOSINOPHILS	Atopic dermatitis
3	46	F	LEFT ELBOW	Intensely pruritic erythematous eczematous patches and plaques with excoriations on the bilateral elbows and neck; previously biopsied outside as spongiotic dermatitis with perivascular neutrophils and eosinophils while on PO steroids.	SPONGIOTIC DERMATITIS WITH EOSINOPHILS	Atopic dermatitis
4	6	F	LEFT ANTERIOR THIGH	Nummular patch	SPONGIOTIC DERMATITIS	Atopic dermatitis
5	20	M	LEFT ELBOW	Eroded erythematous papules	SPONGIOTIC DERMATITIS	Chronic eczematous dermatitis
6	29	F	BACK	Longstanding eczema	SPONGIOTIC DERMATITIS	Chronic eczematous dermatitis
7	29	F	LEFT ANKLE	History of atopic dermatitis	SPONGIOTIC DERMATITIS	Chronic eczematous dermatitis
8	16	M	RIGHT FOREARM	Eczematous rash and itching, worsening	SPONGIOTIC DERMATITIS	Atopic dermatitis
9	86	F	RIGHT BREAST	Itchy bumps on chest and back with erythematous thin papules with central erosions	SPONGIOTIC DERMATITIS	Chronic eczematous dermatitis
10	45	F	LEFT HIP	Generalized eczematous patch and plaques	SPONGIOTIC DERMATITIS WITH EOSINOPHILS	Chronic eczematous dermatitis
11	39	F	LEFT THIGH	Ill-defined pink papules and plaques and desquamation.	SPONGIOTIC DERMATITIS	Asteatotic dermatitis
12	57	M	RIGHT LEG	Red scaling pruritic rash on lower extremities	SPONGIOTIC DERMATITIS	Atopic dermatitis

n=8	Not Available	Not Available	Not Available	These biopsies were all diagnosed as allergic contact dermatitis based on a combination of the clinical features, including well-delineated erythematous patches or plaques, and the histopathologic features of spongiotic dermatitis.	ALLERGIC CONTACT DERMATITIS	Allergic contact dermatitis
n=21	Not Available	Not Available	Not Available	Symptom-free, no history of AD or any other atopic or chronic disease.	NORMAL SKIN	Normal skin

Supplemental Table 4. Characteristics of patients whose skin samples were analyzed for RABGEF1 and MYD88 expression in Figure 9, B-E.